PMM/ A-17

COMISION NACIONAL DE ENERGIA ATOMICA
DEPENDIENTE DE LA PRESIDENCIA DE LA NACION

QUINTO CURSO PANAMERICANO DE METALURGIA

Dentro del Programa Multinacional de Metalurgia
(Programa Regional de Ciencia y Tecnología - OEA)

METALLURGICAL APPLICATIONS OF TRANSMISSION ELECTRON MICROSCOPY

L.M. Brown
(Universidad de Cambridge, Inglaterra)

Departamento de Metalurgia
Buenos Aires - Argentina
1969

Metallurgical Applications of Transmission Electron Microscopy

L. M. Brown

Outline Notes for Lectures given in Buenos Aires, Nov 1969.

Introduction: These notes are largely based on the book "Electron Microscpy of Thin Crystals" by P. B. Hirsch, A. Howie, R. B. Nicholson, D. W. Pashley, and M. J. Whelan, published by Butterworths 1965. Any serious student of the subject, or indeed any user of electron microscopy is urged to have access to this book.

These notes are not meant to be self-explanatory; they are intended to complement the lectures.

§ The Electron Microscope

§1.a Lenses and Elementary Optics

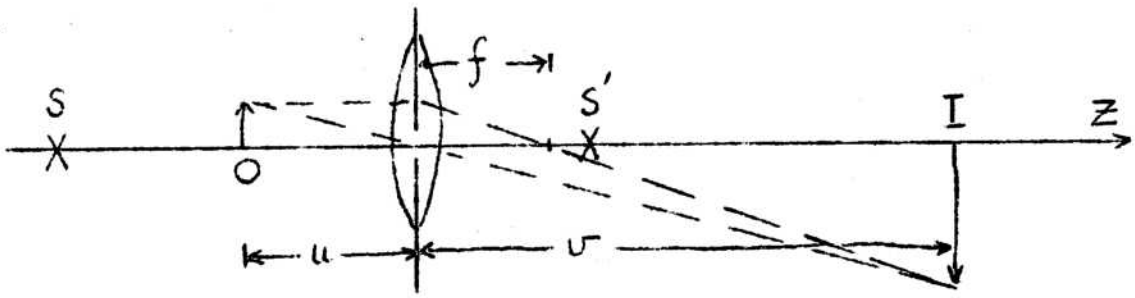

A point source of electrons (light) illuminates an object behind a convergent lens L. A real, inverted image of the object is produced, with magnification v/u where

$$\frac{1}{u} + \frac{1}{v} = \frac{1}{f}$$

Also, an image of the source is produced at S'. If the source is very distant from the lens, S' will approximately coincide with the "back focal point" P of the lens. Furthermore, if the source is far enough from the

object so that the object lies within one Fresnel zone of the waves originating at the source, then the image at S' is the Fraunhofer diffraction pattern of the object. For this reason the plane containing S' is sometimes referred to as the Fourier plane. (see Lipson and Lipson, Optical Physics, C.U.P. 1969).

§1-b Electron Lenses: principle of operation.

Any cylindrically symmetric magnetic field acts to focus electrons. The geometry is given in the figure

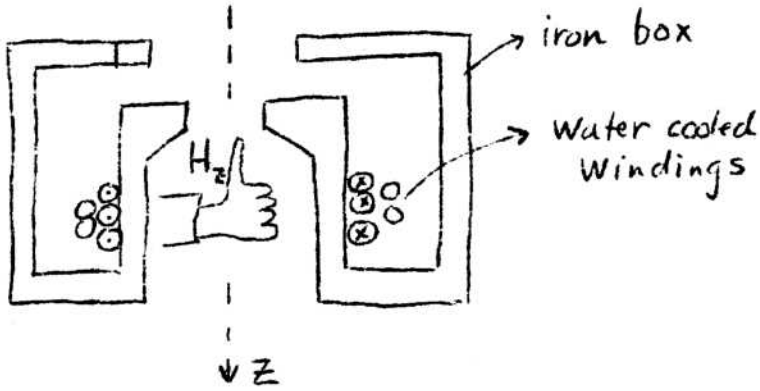

In the "thin lens" approximation, such a lens produces a rotation of the inverted image $\Delta\theta$, where

$$\Delta\theta = -\frac{e}{2mcv_z}\int_{z_{object}}^{z_{image}} H_z\, dz$$

[e = electron charge, m = electron mass, v_z = electron velocity]

and it has a focal length given by

$$\frac{1}{f} \doteq \left(\frac{e}{2mcv_z}\right)^2 \int_{-\infty}^{\infty} H_z^2\, dz \qquad \propto I^2/\Phi$$

Thus the focal length gets shorter (the lens gets stronger) as the current in the windings, I, is increased, and as the accelerating voltage Φ is decreased.

Electron lenses of necessity suffer from spherical aberration, such that rays leaving the object at an angle α to the axis are brought to a focus closer to the lens. The size of the image of an axial point formed from such rays is given by $M\, c_s\, \alpha^3$, where c_s is of the order of the focal length of the lens; say f/3 for a good lens. Thus lenses must be stopped down to achieve good resolution.

The resolution of the microscope is limited because the size of aperture cannot be reduced indefinitely to minimise the spherical aberration. The Rayleigh resolution limit requires the largest possible aperture, and a compromise aperture size must be used.

Operation of the Microscope

§1.c The electron microscope is thus a powerful instrument, for both microscopy and diffraction can be done. Information from micrographs is increased many times by simultaneous electron diffraction experiments. ALWAYS TAKE A DIFFRACTION PATTERN FOR EACH MICROGRAPH. The cost of the extra plate is minimal!

§2. Electron Waves

§2a. Introduction to waves

Electrons obey the Schrödinger wave equation

$$-\frac{\hbar^2}{2m}\nabla^2\psi + V\psi = E\psi$$

If we consider solutions when V is just a constant, we can have plane waves

$$\psi = \text{c.nst.}\ e^{2\pi i\, \underline{k}\cdot\underline{r}}$$

where $k = 1/\lambda = \sqrt{2m(E - V)}/h$

Now (E-V) is the electron s kinetic energy, and can be related to the accelerating voltage in the microscope:

$$\lambda = 12.26/\sqrt{\Phi} \quad \text{in Å , or}$$

$$\lambda = 12.26/\sqrt{(1 + .9788 \times 10^{-6}\Phi)} \text{ in Å , relativistically correct.}$$

We can also have spherical waves

$$\psi = \text{const.}\ \frac{1}{r}\, e^{2\pi i k r}$$

Electron scattering is treated (as is X-ray scattering) by imagining that a plane wave is incident on a scattering center (a speck of dust) and the scattering center is the origin of a weak spherical wave. The spherical wave is thus induced by the incident plane wave. The wave function

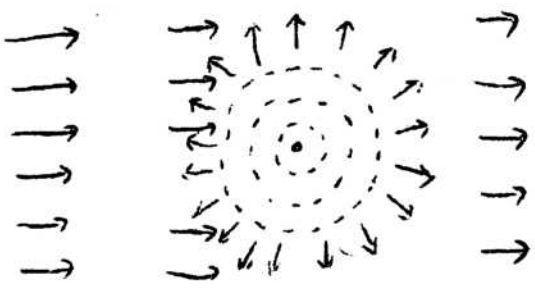

is then written

$$\psi = \psi_{\text{incident}} + \psi_{\text{scattered}} = e^{2\pi i\, \underline{k}\cdot\underline{r}} + f(\theta)\, \frac{e^{2\pi i k r}}{r}$$

where $f(\theta)$ is the "form factor". We will show that $f(\theta)$ can be related to the tabulated X-ray scattering factors, $F_{tab}(\theta)$, by

$$f(\theta) = \frac{me^2}{2h^2} \left(\frac{\lambda}{\sin\theta}\right)^2 (Z - F_{tab}(\theta))$$

Electron scattering factors are approximately 10^4 greater than X-ray scattering factors, because the electrostatic interaction between electrons is much larger than the interaction between an electromagnetic wave and an electron; the ratio of the interactions is approximately $(137)^2$.

Now the fastest and most elegant derivation of the dynamical theory of diffraction would at this point return to Schrödinger's equation. However, it is really more picturesque and useful to follow the X-ray crystallographer's treatment, with which we may be more familiar.

§2b. Scattering of Electrons by Assemblies of Atoms

If we have a lattice, with translation vectors $\underline{t}_n$, the scattered wave with wave vector k' is given by

$$\psi_{\text{scattered}} = \frac{e^{2\pi i k r}}{r}\, F(\theta) \sum_n e^{-2\pi i \underline{k}'\cdot\underline{t}_n}$$

The scattered wave amplitude will be a maximum when $\underline{k}'$ coincides with $\underline{g}$, a reciprocal lattice vector. Some properties of the reciprocal lattice:

(the student is recommended to study Barrett's book, for example, if he is unfamiliar with this).

1) It is formally defined by $\underline{a}^+ = \frac{\underline{b} \times \underline{c}}{V_c}$, $\underline{b}^+ = \frac{\underline{c} \times \underline{a}}{V_c}$, etc.

Here $\underline{a}$, $\underline{b}$, $\underline{c}$ are the base vectors of the real lattice, and $\underline{a}^+$, $\underline{b}^+$, $\underline{c}^+$ of the reciprocal lattice.

2) only if $\underline{a} \perp \underline{b} \perp \underline{c}$ is $\underline{a} \parallel \underline{a}^+$, etc.

3) the reciprocal of the reciprocal lattice is the real lattice.

4) The distance between equivalent planes with Miller indices h,k,l d_{hkl} is

$$d_{hkl} = \left| h\underline{a}^+ + k\underline{b}^+ + l\underline{c}^+ \right|^{-1}$$

5) Any function which is periodic in the real lattice can be Fourier analysed in terms of reciprocal lattice vectors; e.g., the potential energy due to the atoms

$$V(\underline{r}) = \sum_{\underline{g}} V_{\underline{g}} \, e^{2\pi i \underline{g}.\underline{r}}$$

where

$$V_{\underline{g}} = \frac{1}{V_c} \int_{\text{unit cell}} V(\underline{r}) \, e^{-2\pi i \underline{g}.\underline{r}} \, d^3\underline{r} \, .$$

6) For the reciprocal lattice construction in hexagonal crystals, and how to handle Miller indices in these crystals, the student is recommendsed to read F. C. Frank, Acta. Cryst. 18 (1965) 862.

Thus one is led to the famous Ewald sphere construction to represent the geometry of diffraction. This construction enables one to solve complicated

diffraction problems with considerable ease. In general, diffraction from an object produces intensity distributions in reciprocal space which are closely related to the shape of the object, being streaked in directions perpendicular to small dimensions of the object.

The structure factor $F(\theta)$ can be calculated from atomic scattering factors:

$$F(\theta) = \sum_i f_i(\theta)\, e^{-2\pi i \underline{g} \cdot \underline{r}_i}$$

where $\underline{r}_i$ denotes the position of an atom in the unit cell, and the sum is taken over atoms in the unit cell.

§2c. Extinction Distance

The extinction distance is a measure of the strength of the scattering of electrons by the lattice. It is, roughly speaking, π times the distance in which an incident beam would be completely diffracted away, if double diffraction did not occur. It thus measures the importance of the phenomenon called "primary" extinction in X-ray crystallography.

The fundamental relationship can be derived by calculating ψ_{scatt} due to a slab of scattering material. If the thickness of the slab is t, one finds for the amplitude scattered with wave vector k' inclined at θ to the normal to the slab:

$$\psi_{scatt} = \frac{i \lambda F(\theta) t}{V_c \cos \theta}\, e^{2\pi i \underline{k}' \cdot \underline{r}}$$

In particular, in the forward direction ($\theta = 0$):

$$\psi_{scatt} = \frac{i \lambda F(0)}{V_c}\, t\, e^{2\pi i k z} = \frac{i\pi}{\xi_0}\, t\, e^{2\pi i k z}$$

and in the Bragg direction ($\theta = \theta_B$)

$$\psi_{scatt} = \frac{i \lambda F(2\theta_B)}{V_c \cos 2\theta_B} \; t \; e^{2\pi i(\underline{k} + \underline{g}).\underline{r}} = \frac{i\pi}{\xi_g} t \; e^{2\pi i(\underline{k} + \underline{g}).\underline{r}}$$

These equations define the extinction distances for forward and Bragg scattering, respectively.

The extinction distance is:

1) inversely proportional to $F(\theta)$; i.e. the more strongly the electrons interact with the crystal, the shorter is ξ_g ;
2) approximately proportional to g^2 for g large; thus the extinction distance increases with increasing order of reflection (although there be irregular variation due to structure factor effects);
3) approximately proportional to the square root of the accelerating voltage;
4) generally a decreasing function of atomic number.

§2d. Kinematical Theory

If we let $\underline{k}' = \underline{k} + \underline{g} + \underline{s}$, where $\underline{s}$ represents the deviation of the perfect crystal from the Bragg reflecting position, and if further, we let the atoms be displaced from their positions in the perfect crystal by a displacement vector $\underline{R}$, then

$$\psi_{scatt} = \frac{i\pi t}{\xi_g} e^{-2\pi i(sz + \underline{g}.\underline{R})} \; e^{2\pi i(\underline{k} + \underline{g}).\underline{r}}$$

$$= \mathcal{S}\phi_g \; e^{2\pi i(\underline{k} + \underline{g}).\underline{r}}$$

Thus the amplitude scattered into the Bragg reflection can be found by summing over all slabs: one finds

$$\Delta \phi_g = \frac{i\pi}{\xi_g} \int_{z=0}^{t} e^{-2\pi i(sz + \underline{g}\cdot\underline{R})}\, dz$$

§2e. Consequences of the Kinematical Theory

1) If $\underline{R} = 0$ or $\underline{R} = \text{const}$, one finds

$$\left|\Delta\phi_g\right|^2 = \left(\frac{\pi}{\xi_g}\right)^2 \frac{\sin^2 \pi t s}{\pi^2 s^2}$$

which predicts thickness fringes, and bend extinction contours.

2) The integral represents an amplitude phase diagram.

3) If $\underline{R}$ is a function of z, contrast will be generated.

§ 3 The Dynamical Theory of Electron Propagation

§ 3.a The Dynamical Theory is so-called because it describes the dynamical equilibrium between the direct and diffracted beam. Mutual coupling occurs by each beam scattering into the other. From what we already know,

$$\left.\begin{aligned} \frac{d\phi_g}{dz} &= \frac{i\pi}{\xi_o}\phi_g + \frac{i\pi}{\xi_g}\phi_o \; e^{-2\pi i(sz + \underline{g}.\underline{R})} \\ \frac{d\phi_o}{dz} &= \frac{i\pi}{\xi_o}\phi_o + \frac{i\pi}{\xi_g}\phi_g \; e^{2\pi i(sz + \underline{g}.\underline{R})} \end{aligned}\right\} \quad \text{H.W 1}$$

These equations can be put into a number of equivalent forms. The most useful from the defect point of view is found by putting

$$\phi_g'' = e^{2\pi i(sz + \underline{g}.\underline{R})} \; e^{-i\pi z/\xi_o}\phi_g$$

$$\phi_o'' = e^{-i\pi z/\xi_o}\phi_o$$

and getting

$$\left.\begin{aligned} \frac{d\phi_o''}{dz} &= \frac{i\pi}{\xi_g}\phi_g'' \\ \frac{d\phi_g''}{dz} &= \frac{i\pi}{\xi_g}\phi_o'' - 2\pi i\left(sz + \frac{d}{dz}(\underline{g}.\underline{R})\right)\phi_g'' \end{aligned}\right\} \quad \text{H.W 3}$$

It is clear from H.W. 3 that the presence of the defect changes the local value of s, and that $(\Delta s)_{local} = \frac{d}{dz}(\underline{g}.\underline{R}) = \beta'$. This local change can be viewed from the point of view of elasticity as the sum of the symmetrical shear strain and the rotation: i.e. the contrast arises <u>both</u> from strains and from local rotations. The contrast depends on bending of the Bragg planes.

The perfect crystal solution of equations H-W 1 or H-W 3 can be viewed in a number of ways.

1) Consider s = o. Then the amplitudes ϕ_o and ϕ_g oscillate symmetrically with period $\xi_g/2$. They "each drive the other". For this case,

$$\phi_o = e^{i\pi z/\xi_o} \cos \frac{\pi t}{\xi_g}$$

$$\phi_g = e^{i\pi z/\xi_o} \, i \sin \frac{\pi t}{\xi_g}$$

2) Consider S large, or t small. Then the kinematical theory is recovered.

3) An amplitude-phase diagram can be constructed to calculate ϕ_g. It has a radius $(\xi_g^{-2} + s^{-2})^{-\frac{1}{2}}$ so that the limiting radius for s = o is ξ_g^{-1}. This is of great interest, because ξ_g^{-1} then represents the limiting size of the intensity distributions in reciprocal space for infinite perfect crystals.

4) The solutions may also be represented using "normal modes". The normal modes in this case are Bloch waves, with wave vectors lying on each of two branches of the dispersion surface.

§ 3.b Absorption

The theory is still not quite complete, in that the thickness fringes die away with depth. Clearly some "damping" must be put into the theory. We put

$$1/\xi_g \rightarrow 1/\xi_g + i/\xi_g'$$

$$1/\xi_{\bar{g}} \rightarrow 1/\xi_{\bar{g}} + i/\xi_{\bar{g}}'$$

These expressions can be put into all our previous work so that, for instance, using

$$\cos(ix) = \cosh x$$

$$\sin(ix) = i \sinh x$$

we find, for the perfect crystal with $s = 0$,

$$\phi_0 \rightarrow e^{-\pi z/\xi_0'} e^{i\pi z/\xi_0} \cos\frac{\pi t}{\xi_g} \cosh\frac{\pi t}{\xi_g'} - i \sin\frac{\pi t}{\xi_g} \sinh\frac{\pi t}{\xi_g'}$$

$$\phi_g \rightarrow e^{-\pi z/\xi_0'} e^{i\pi z/\xi_0} \sin\frac{\pi t}{\xi_g} \cosh\frac{\pi t}{\xi_g'} + i \cos\frac{\pi t}{\xi_g} \sinh\frac{\pi t}{\xi_g'}$$

From these expressions, we find that as $t \rightarrow \infty$,

$$|\phi_0|^2 \rightarrow \tfrac{1}{2} e^{2\pi t \left(\frac{1}{\xi_g'} - \frac{1}{\xi_g}\right)}$$

$$|\phi_g|^2 \rightarrow \text{the same.}$$

Thus the fringes disappear, in accord with experiment.

§ 3.c Analogues of the Dynamical Theory

1. The coupled pendulum.

2. The wave guide.

§§ 3.d Relation between the dynamical theory and the Nearly Free Electron Model of Solid State Physics.

(The reader should consult, for example, a standard text on Solid State Physics)

In discussing the band structure of crystals, one usually solves the Schrödinger equation for a one-dimensional periodic potential $V_g \sin 2\pi g n$, and one finds that there is a forbidden range of energies at $k_x = g/2$, the range being given by $2V_g$.

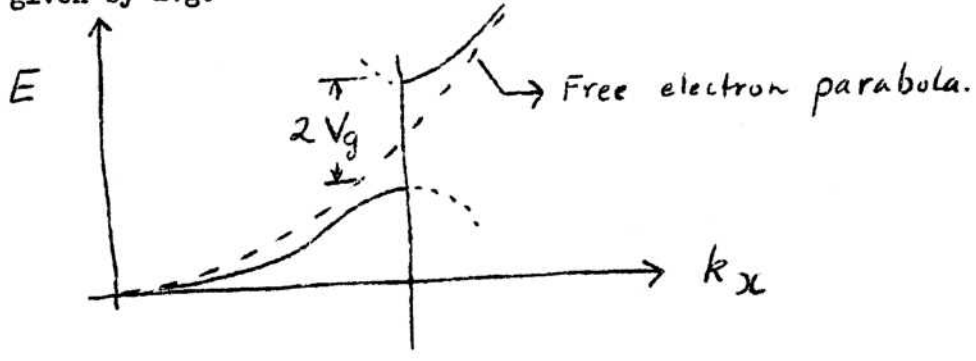

The wave function of the electrons is a Bloch wave, i.e.

$$\psi_k = B_k \, e^{2\pi i \underline{k}\cdot\underline{r}}$$

where B_k is a function with the lattice periodicity. Thus

$$\psi_k = \sum_g B_{kg} \, e^{2\pi i (\underline{k} + \underline{g})\cdot\underline{r}}$$

$$= B_{ko} \, e^{2\pi i \underline{k}\cdot\underline{r}} + B_{kg} \, e^{2\pi i (\underline{k} + \underline{g})\cdot\underline{r}}$$

in the two beam case.

In the case of interest to us, the <u>total</u> energy of the electron is fixed by the accelerating voltage. However, when the crystal is oriented for Bragg reflection ($K_x = g/2$) one finds that the kinetic energy of the crystal may take on one of two values, E_1 or E_2. Corresponding to these values are two values of the k-vector, k_1 and k_2 where

$$E_2 = \frac{h^2 k_2^2}{2m} \; ; \qquad E_1 = \frac{h^2 k_1^2}{2m} \; .$$

Now $\Delta k = k_2 - k_1$ is very small by comparison with either k_1 or k_2, and we find

$$\Delta E = E_1 - E_2 = 2V_g \; ; \quad \Delta k = k_1 - k_2 = \frac{2mV_g}{h^2}$$

But $\Delta k = (\xi_g)^{-1}$, as we have seen. The physical picture for this is that at the Bragg position, two curves may exist in the crystal: one wave with <u>peaks</u> at the atomic positions ($B_{ko} = B_{kg}$) and one wave with <u>valleys</u> at these positions ($B_{ko} = - B_{kg}$). Thus the waves represent states with different kinetic energies.

In the complete theory, the Bloch waves are written

$$\psi_{k1} = C_{o1}\, e^{2\pi i \gamma_1 z}\, e^{2\pi i \underline{k}\cdot\underline{r}} + C_{g1}\, e^{2\pi i \gamma_1 z}\, e^{2\pi i (\underline{k}+\underline{g})\cdot\underline{r}}$$

and $$\psi_{k2} = C_{o2}\, e^{2\pi i \gamma_2 z}\, e^{2\pi i \underline{k}\cdot\underline{r}} + C_{g2}\, e^{2\pi i \gamma_2 z}\, e^{2\pi i (\underline{k}+\underline{g})\cdot\underline{r}}$$

The "wave" theory and the "Schrodinger" theory are thus identical.

§ 4. Methods of Computing Images

§4.a Stacking Faults, etc.

For defects with $\underline{g}\cdot\underline{R}$ which varies in a step, the problem is best done by wave-matching.

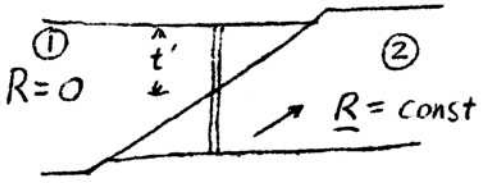

If we inspect the H-W equations, we find that th ere will be a discontinuity in the derivatives of ϕ_o and ϕ_g whenever there is a discontinuity in R. For instance, if we call $\alpha = 2\pi\, \underline{g}\cdot\underline{R}$ we find

$$\left[\frac{d\phi_o}{dz}^{(2)} - \frac{d\phi_o}{dz}^{(1)}\right]_{\text{at } z=t'} = \frac{i\pi}{\xi_g}\, e^{2\pi i s t'} \left[\phi_g^{(2)}\, e^{i\alpha} - \phi_g^{(1)}\right]_{\text{at } z=t}$$

and similarly for ϕ_g .

Now if there is a step discontinuity in the first derivative, the functions

themselves must be continuous. Thus

$$\phi_o^{(2)} = \phi_o^{(1)} \quad \text{at} \quad z = t'$$

and similarly for ϕ_g .

The wave-matching can now be carried out exactly as in elementary wave mechanics or electromagnetism. For the example of the stacking fault depicted above, at s = o, a short calculation gives

$$\left|\phi_o^{(2)}\right|^2 = \cos^2 \frac{\pi z}{\xi_g} - 2 \sin\alpha \sin\frac{\pi t'}{\xi_g} \cos\frac{\pi z}{\xi_g} + 4\sin^2\alpha/2 \sin^2\frac{\pi t'}{\xi_g}.$$

Absorption can be included as described above.

This type of calculation can be made routine for several layers of faults by using matrix methods, although it is not clear to me that any great saving in effort is achieved if only two layers are to be considered. If more than two layers are involved, the matrix method can be set up on the computer, using standard matrix sub-routines.

Discontinuities in the derivatives arise if a) there is a displacement, as at a stacking fault or precipitate; b) the structure factor changes suddenly, as in a precipitate; or c) the value of s changes suddenly. These latter fringes are called "s-shift" or δ - fringes.

§ 4b. Defects with continuous displacement fields

For this case, the differential equations must be integrated. There are three problems:

i) To find the displacement field of the defect.

For dislocation configurations, this is most conveniently done using

the "infinitesimeal loop" method. If we have a loop of area δA, so that

$$D = \frac{b \delta A}{8\pi(1-\nu)}$$

and it is a prismatic loop, with normal $\underline{u} = (0,0,1)$ and Burgers vector $\underline{b} = (0,0,b)$ then it gives rise to displacements

$$U_x = \frac{D}{r^2} \left[-(1-2\nu) x/r + 3Xz^2/r^3 \right]$$

$$U_y = \frac{D}{r^2} \left[-(1-2\nu) y/r + 3yz^2/r^3 \right]$$

$$U_z = \frac{D}{r^2} \left[(1-2\nu) \frac{z}{r} + 3z^3/r^3 \right]$$

if it is a Shear loop, with normal $\underline{u} = (0,0,1)$ and Burgers vector $\underline{b} = (b,0,0)$ then it gives rise to displacements

$$U_x = \frac{D}{r^2} \left[(1-2\nu) z/r + 3x^2 z/r^3 \right]$$

$$U_y = \frac{D}{r^2} \left[3xyz/r^3 \right]$$

$$U_z = \frac{D}{r^2} \left[(1-2\nu) x/r + 3xz^2/r^3 \right].$$

From these expressions, $\underline{R} = \underline{i} u_x + \underline{j} u_z + \underline{k} u_z$ can be found for any configuration of dislocations by synthesis. Examples will be given to show how this may be done. Usually, a separate sub-routine is needed to calculate a table of α-values.

Surface corrections can easily be inserted using the method of Cheng. An example will be given.

ii) The second problem concerns the integration of the differential equations. Usually a standard library routine exists for this.

Great efficiency in the use of computer time can be achieved using the method of Head (Aust. J. Phys. 20 (1967) 557). This method enables the contrast to be calculated for any depth of the defect in the foil with only one integration of the differentail equations.

iii) The third problem to be tackled is the presentation of the data. Early papers used graphical methods, but (largely by virtue of Head's time-saving technique) it is now possible to print an intensity map directly, and so to convey a great deal of information easily.

To summarise, the complete program looks something like this:

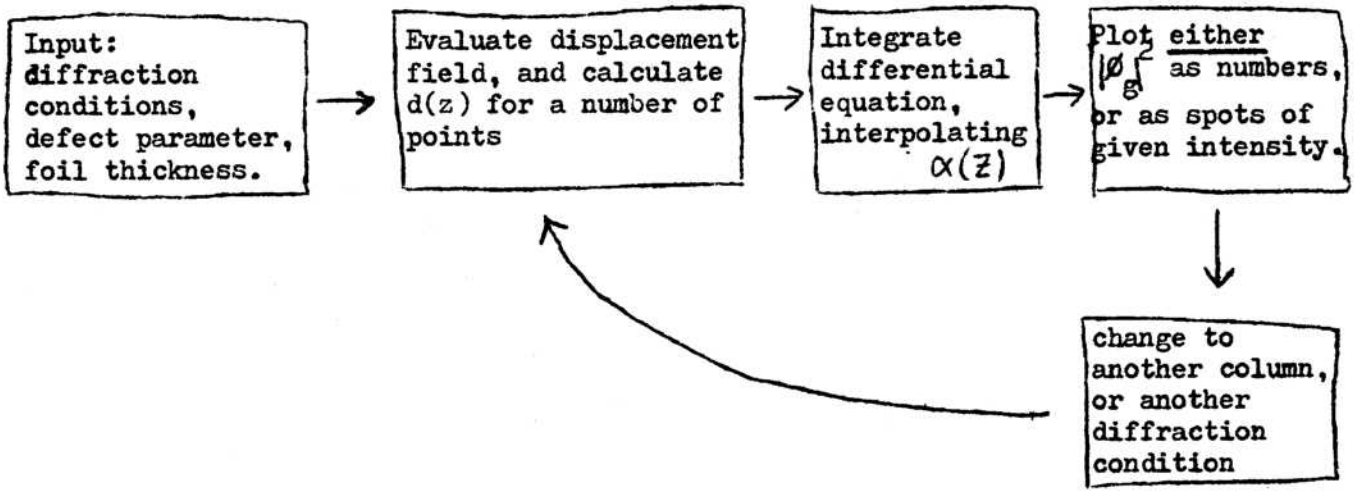

§5. General Principles of Contrast from Defects, or what can be done without computing

There are two main sources of contrast. The first depends entirely upon local changes in orientation, thickness, structure-factor, etc., and will exist even if the atoms in a given column suffer no displacement gradients. Thickness fringes, or contrast arising from misorientations at grain boundaries are examples. Usually a knowledge of the rocking-curve will suffice to interpret such contrast.

The second type of contrast depends upon the existence of displacement gradients. It is characterized by the existence of fringes, of spacing $\xi_g / \sqrt{1 + w^2}$. These fringes arise from the periodic alternation of direct and Bragg intensity. The fringes are weak when the defect is in the center of the foil. A further characteristic of this sort of contrast is the Bright-Field and Dark-Field images are similar, if the defect is near the bottom (electron-exit) surface of the foil.

Most defects give rise to both types of contrast.

§ 6. Fringes

Fringes arise whenever two plane waves, travelling in slightly different directions, are recorded on a photographic plate or fluorescent screen. If we assume the z-component of the wave-vectors is the same, and the wave-vectors differ by a small amount

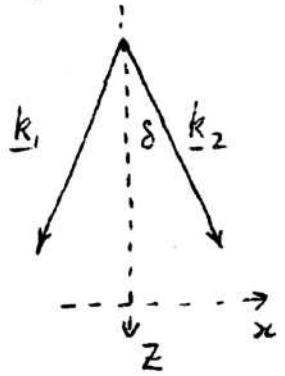

in their x-components, so that

$$\underline{k}_1 = (-\delta k, o, k); \quad \underline{k}_2 = (\delta k, o, k)$$

then $\underline{A} = e^{2\pi i \underline{k}_1 \cdot r} + e^{2\pi i \underline{k}_2 \cdot \underline{r}} = (\text{a phase factor})(\sin 2\pi\delta k$

Thus the intensity ($= A^2$) has a periodicity of $\frac{1}{2\delta k}$ in the x-direction. The fringes appear as stripes perpendicular to the plane containing the two wave-vectors. These fringes are exactly the same as two-beam interference fringes in optics, as are, for example, to be found in a Young's slit experiment.

In a qualitative way, without detailed computing, one can establish the following types of fringes:

In a qualitative way, without detailed computing, one can establish the following types of fringes:

TYPE	SPACING	VISIBILITY	SPACING DEPENDS ON S?	REFERENCES
attice esolution	... d_{hkl}	whenever intensity in both $\phi_o \mathcal{E} \phi_g$	no	HHNPW Ch.15.1
›iré	$\left[\left(\frac{1}{d_1} - \frac{1}{d_2}\right)^2 + \frac{4\sin^2\theta/2}{d_1 d_2}\right]^{-\frac{1}{2}}$	whenever intensity in both g_1 and g_2	no	HHNPW Ch.15; Gevers P.M.7 (1962)1681
tacking-ault or displacement ringe"	$\frac{\text{depth}}{\xi_g/\sqrt{1+\omega^2}}$ periodicity	best at s=o	yes	HHNPW Ch.10
tructure-actor	$\frac{\text{depth}}{\sim \xi_g/\sqrt{1+\omega^2}}$ periodicity	invisible at s=o	yes	HHNPW Ch.10.6 (cavity)
-shift or δ - fringes	irregular, but $\sim \xi_g$	best for $S_1 = -S_2$	yes	Gevers et.al. phys.stat.sol. 4(1964)383 and 5(1964)595
hickness ringes	$\xi_g/\sqrt{1+\omega^2}$	best at s = o	yes	

In addition, there are types which have not been adequately studied, such as fringes at grain boundaries. Using the principles outlined above, certain qualitative predictions can be made about these.

§ 7. Detailed Discussion of Contrast from Stacking-Faults, Dislocations, and Inclusions

§ 7(a). Stacking Faults

Consider f.c.c. case, to start with.

Two types of fault exist, intrinsic and extrinsic. An intrinsic fault is caused by motion of a single shockley partial dislocation (involving shear on one plane only) or by condensation of vacancies. An extrinsic fault is caused by the motion of a shockley partial which involves synchronous shear on two adjacent planes, or by the condensation of interstitials.

The Burgers vector of a Shockley partial dislocation is $\frac{1}{6}\langle 121 \rangle$, so that $\alpha = 2\pi g.R = \frac{\pi}{3}(h + 2k + 1)$. In the f.c.c. lattice, allowed reflections are those for which h, k, l are either all even or all odd, so $\alpha = 0, \pm \pi/3, \pm 2\pi/3, \pm 2\pi$ etc. are the values of α. For a given geometry, an extrinsic fault and an intrinsic fault will have a different sign of α. It is also worth noticing that any translation vector of the lattice can be added to R so that if $\underline{t} = \frac{1}{2}\langle 101 \rangle$ is added to $\frac{1}{6}\langle 121 \rangle$, R becomes $\frac{1}{3}\langle 111 \rangle$: i.e., the $\underline{R}$-vector for the fault can be equivalently a vector lying in the fault plane, or a vector normal to the fault plane. In the case of slip by shear, it is convenient to think of the former description, but in the case of vacancy condensation, it is convenient to think of the latter description.

From the previous work, we see that a stacking fault will give rise to fringes of depth periodicity $\xi_g / \sqrt{1 + \omega^2}$; that the bright-field image will be symmetrical about the center line, and the dark-field image "antisymmetrical", and that the fringes will be weak in the center of the foil. Quite good agreement between theory and experiment can be achieved.

The type of stacking fault can be determined, using the following rule: In reasonably thick absorbing crystals ($t > 3\,\xi_g$), with g and the fault-plane making acute angles, a fault is <u>intrinsic</u> if the fringe arising from the top of the foil is brighter than background. A short-hand method of making experimental determinations of the intrisnic or extrinsic nature of faults has been given by Gevers et. al. (Phys. stat. sol. <u>3</u> (1963) 1563).

An interesting question arises in the observation of <u>overlapping</u> faults. Suppose two faults of opposite α lie on planes separated by a distance d : how close can they be before the image disappears? A simple amplitude-phase diagram suggests that d should be greater than about $\xi_g/50$ for visibility. The question is discussed by Booker & Howie (Applied Physics Letters <u>3</u> (1963) 156). Booker & Howie point out that overlapping faults will give rise to images which are not symmetrical in bright-field.

A related question is the minimum value of α which is necessary to ensure visibility. Howie and Jouffrey (Phil. Mag. <u>14</u> (1966) 201) claim $\alpha \gtrsim .02$ for visibility. In this way, they were able to set limits on the displacement of the atomic planes in a direction perpendicular to the fault in cadmium.

In materials other than f.c.c., values of $\alpha = \pi$ can be found. These can be produced in ordered material, when they are "anti-phase boundaries", (see Fisher and Marcinkowski, Phil. Mag. 6 (1961) 1385). Also in certain layer structures (Drum and Whelan Phil. Mag. 11 (1965) 205) these faults have been found. They are characterised by a set of fringes which does not interact with thickness fringes.

The value of the stacking-fault energy can be determined in a number of favourable cases. Two main direct methods exist:

1. Whelan's method. In this method, the size of dislocation nodes in networks is measured to yield the stacking fault energy. Brown and Thölen (Discuss. Faraday Soc. 38 (1964) 35) describe how this may be done.

2. Observation of Intrinsic-Extrinsic Fault Pairs. In this method, first employed by Gallagher (Phys. Stat. Sol. 16 (1966) 95); a particularly simple dislocation-fault configuration is used to calculate fault energies.

In cases where the two methods have been compared the derived stacking-fault energies agree to within experimental error.

§ 7(b) Other types of Fringes

Quantitative expressions for contrast from Moire fringes can be obtained from the equations for stacking faults simply by letting the displacement vector $\underline{R}$ become a function of distance in the interface. If $\underline{R} = -\frac{|\Delta g|}{|g|}\, x$, then $\alpha = -2\pi \underline{\Delta g}.\underline{x}$, where x is a vector lying in the interface. Thus the fringes (loci of constant α) are perpendicular to $\underline{\Delta g}$ and have a spacing

proportional to $|\Delta g|^{-1}$. This treatment (after Gevers, Phil. Mg. 7 (1962) 1681) is to be compared with that in the preceding section.

If there is a change in S on crossing the interface, $\mathcal{S}$- fringes or S-shift fringes result. Calculation gives the characteristics listed in the previous section. Comparison with experiment has been made in the case of ferro-electric anti-phase boundaries in barium titanate (Gevers, Delavignette, Blank, Van Landuyt and Amelinckx, phys. stat. sol. 5 (1964) 595), and at twin boundaries in a V_3Si alloy at low temperatures (Goringe and Valdre, Proc. Roy. Soc. A295 (1966) 192). The effect is also of importance at any planar coherent interface due to elastic strains (Ardell, Phil. Mag. 16 (1967) 147).

§ 7(b) Dislocations

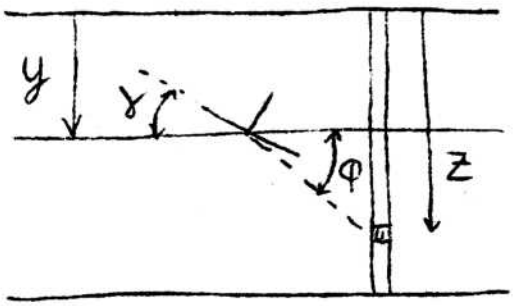

For the co-ordinate system shown, standard dislocation theory in an isotropic continuum gives

$$\underline{R} = \frac{1}{2\pi}\left\{\underline{b}\,\bar{\Phi} + \underline{b}_e\,\frac{\sin 2\Phi}{4(1-\nu)} + \underline{b}\times\underline{u}\left(\frac{(1-2\nu)}{2(1-\nu)}\log|\underline{r}| + \frac{\cos 2\Phi}{4(1-\nu)}\right)\right\}$$

when ν is Poisson's ratio, $\Phi = \varphi - \gamma$, $\underline{b}$ is the total Burgers vector, $\underline{b}_e$ is the edge component of $\underline{b}$, and $\underline{u}$ is a unit vector along the dislocation line.

There are two points to be noted:

1) for a screw dislocation, $\underline{b}_e = \underline{b} \times \underline{u} = o$, and if $\underline{g} \cdot \underline{b} = 0$, no contrast will be observed. This is the famous vanishing criterion of Hirsch, Howie and Whelan. This means that $\underline{g}$ is perpendicular to the dislocation line.

2) for an edge dislocation, the vanishing criterion is $\underline{g} \cdot \underline{b} = 0$, and $\underline{g} \cdot (\underline{b} \times \underline{u}) = o$. This means that $\underline{g}$ is parallel to the dislocation line.

Thus it is possible in principle to determine the Burgers vectors of dislocations by carrying out "contrast" experiments. In doing this work, it is necessary to have both a good tilting stage, and a computer programme to compare observed and calculated images. The reason for this is that dislocations effectively "vanish" if $\underline{g} \cdot \underline{b} \leq 1/3$, as well as in dark-field conditions when $S \neq o$ (see France and Loretto, Proc. IV European Regional Conference on Electron Microscopy Rome 1968). In order to have a convincing determination, quite detailed comparison is desirable.

The sense of the Burgers vector of a dislocation loop can be determined by appropriate tilting experiments. The principle of the method can be shown in the diagram, using the arguments presented by Groves and Kelly (Phil. Mag. 6 (1961) 1527 ; also Phil. Mag. 7 (1962) 892). The arrows show the sense of the local rotation for a vacancy loop; clearly, if the diffraction conditions are such that a clockwise rotation fringes the crystal into the reflecting position, the image is inside the loop, and vice-versa.

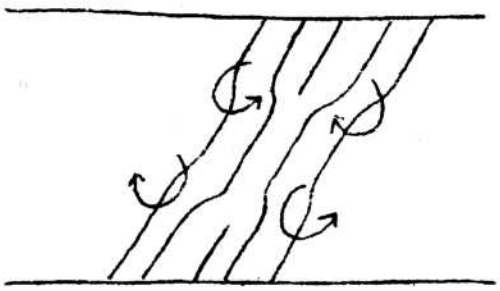

A short and method based on this principle has been devised by Edmondson and Williamson (Phil. Mag. 9 (1964) 277).

§7(c) Inclusions

In this case, by "inclusion" we mean any defect which has a three-dimensional strain-field or shape. Vacancies, gas-bubbles, and gross precipitates are all "inclusions" in this sense.

Inclusions are rendered visible by a number of mechanisms:

1) Structure-Factor, or "Thickness" contrast:

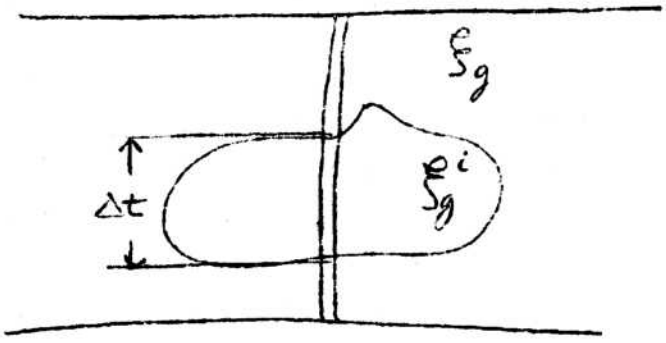

In this contrast mechanism, the inclusion has a scattering power which is different from that of the matrix. This is reflected in a different extinction distance. This case has been treated quite fully by Gleiter (Phil. Mag. 18 (1968) 847); for voids the reader is recommended to read Landuyt, Gevers and Amelinclex (Phys. stat. sol. 10 (1965) 319).

The principle of the contrast can be readily understood when the inclusion is very small, by use of an amplitude phase diagram. There is an effective change in foil-thickness,

$$\Delta t' = \Delta t \left(\frac{1}{\xi_g^i} - \frac{1}{\xi_g} \right)$$

and this gives rise to contrast whenever the transmitted or diffracted intensity

depends strongly on foil-thickness. One finds that the change in transmitted intensity at s = o due to the inclusion is

$$\Delta I = -\pi \Delta t \left(\frac{1}{\xi_g'} - \frac{1}{\xi_g} \right) \sin \frac{2\pi t}{\xi_g} .$$

This formula predicts that very small inclusions can be seen. For instance, if the microscope had perfect resolution, a thickness change corresponding to the removal of a single layer of atoms would be visible.

2) "Interface" Contrast:

In this category we may include all types of fringes, whose production we have already discussed. Moiré fringes, fringes due to displacement at the precipitate, δ-fringes due to coherency strains at a planar interface (Ardell, Phil. Mag. 16 (1967) 147; Weatherly, Phil. Mag. 17 (1968) 647), and the observation of interface dislocations all fall into this category.

The observation of interface dislocations has not yet been adequately treated theoretically. Weatherly and Nicholson (Phil. Mag. 17 (1968) 801) have made some rules for best observation of these dislocations based on their experiments.

3) "Strain" Contrast:

This subject has been treated for two common types of precipitate by Ashby and Brown (Phil. Mag. 8 (1963) 1649). Under favourable circumstances, both the magnitude and sign of the strains can be measured. The visibility of precipitates by this mechanism has also been discussed.

The following points may be noted:

1. For precipitates whose image is wider than approximately an extinction distance, a single rule exists by which the sign of the strain can be determined by dark field micrograph.

2. For small images, the black-white nature of the image reverses every $\xi_g/2$, as in the dislocation case, except that the reversals occur at $\xi_g/4$, $3\ \xi_g/4$, etc. (McIntyre and Brown, J. de Physique, Colloue. C.3, 1966, p. 178).